THE ASTROPHYSICAL JOURNAL, 463:543–554, 1996 June 1

GLOBULAR CLUSTER SYSTEMS IN DWARF ELLIPTICAL GALAXIES. I. THE dE,N GALAXY NGC 3115 DW1

PATRICK R. DURRELL, DEAN E. MCLAUGHLIN, AND WILLIAM E. HARRIS
Department of Physics and Astronomy, McMaster University, Hamilton, Ontario, Canada L8S 4M1; durrell@physun.physics.mcmaster.ca, dean@physun.physics.mcmaster.ca, harris@physun.physics.mcmaster.ca

AND

DAVID A. HANES[1]
Department of Physics, Queens University, Kingston, Ontario, Canada K7L 3N6; hanes@astro.queensu.ca
Received 1995 March 10; accepted 1995 December 15

ABSTRACT

We present new *BV* photometry of the globular cluster system (GCS) around the dE1,N dwarf companion galaxy to NGC 3115. Its GCS has a total population of 59 ± 23 clusters and a mean metallicity $\langle[\mathrm{Fe/H}]\rangle \simeq -1.2 \pm 0.13$, which is about 0.5 dex more metal poor (in the mean) than that of the dE halo light. Neither the GCS nor the galaxy halo exhibits a radial color gradient. We derive a distance modulus $(m - M)_V = 30.3^{+0.8}_{-0.5}$ ($d \sim 11^{+5}_{-2.3}$ Mpc) by using the turnover of the globular cluster luminosity function (GCLF); this result is consistent with the dwarf being a physical satellite of NGC 3115. The specific frequency of NGC 3115 DW1 is $S_N = 4.9 \pm 1.9$, considerably larger than that of NGC 3115 itself, but similar to those of dE's in the Local Group, as well as many large ellipticals. Finally, we find that the GCS mass spectrum follows a power law $dN/dm \sim m^{-1.8}$ above the turnover of the GCLF. This slope is similar to those found in many larger elliptical and spiral galaxies and suggests that the mechanisms of globular cluster formation are similar in galaxies of a large range in mass.

Subject headings: galaxies: individual (NGC 3115 DW1) — galaxies: photometry — galaxies: star clusters — galaxies: structure

1. INTRODUCTION

Dwarf galaxies are by far the most common type of galaxy, yet their small sizes and low surface brightnesses have limited our detailed understanding to only the nearest examples. These galaxies are of great cosmological interest since their progenitors have been postulated to arise naturally in hierarchical clustering models (such as cold dark matter; see Kauffmann, White, & Guideroni 1993) of galaxy formation. Searle & Zinn (1978) proposed that the Milky Way may have formed from a chaotic merger of many such protogalactic fragments, and other recent discussions (e.g., Larson 1990, 1992; Freeman 1993; Zinn 1993) suggest that today's dwarf galaxies may in fact be the leftover "pieces" from this process that evolved in isolation without being absorbed into the larger galaxies. The dwarfs also provide a useful probe into the evolution and dynamics of galaxy clusters, since dwarf ellipticals (dE's) are known to cluster preferentially near large galaxies or near the cores of galaxy clusters (Ferguson & Sandage 1989; Vader & Sandage 1991; see Ferguson & Binggeli 1994 for an excellent review of dE's). Understanding these tiny systems seems essential for an understanding of galaxy formation in general.

A vital clue to how dwarf galaxies formed may lie in their globular cluster systems (GCSs). Much is known about the total numbers, metallicity distribution functions, luminosity distribution functions, and even the dynamics of GCSs in *large* elliptical and spiral galaxies (see Harris 1991a, 1993, 1995 for recent reviews). However, little work has yet been done on GCSs in *dwarf* galaxies. The primary reason for this is simply one of sample size: even a relatively bright dwarf elliptical with a "normal" specific frequency ($S_N \sim 5$) would have only ~ 30 globular clusters. The five most luminous dE galaxies in the Local Group (NGC 147, 185, 205, Fornax, and the Sgr dwarf) have populations from 3 to ~ 10 clusters each (Hodge 1973, 1974, 1976; Ford, Jacoby, & Jenner 1977; Buonanno et al. 1985; Da Costa & Mould 1988; Da Costa & Armandroff 1995). All of these clusters are metal poor and at least superficially resemble those found in the Milky Way halo. Outside of the Local Group, only seven other dE's (mostly in the Virgo Cluster) have been noted as having GCSs (Harris 1991b and references within; Vader & Chaboyer 1994), although none of these has been studied in any detail.

There are now additional motivations for studying GCSs in dwarf galaxies on theoretical grounds. Harris & Pudritz (1994, hereafter HP94; see also McLaughlin & Pudritz 1996) have developed the first stages of a model for globular cluster formation in which clusters form out of the very dense gas cores that build up within giant molecular clouds. However, to attain the characteristic $\sim 10^5$–$10^6 M_\odot$ mass range of globular clusters, the protoclusters must have built up within "supergiant" molecular clouds (SGMCs) very much more massive than the GMCs that we see in the Galactic disk today. In the HP94 model, these SGMCs turn out to have the right size and mass to be identical with the Searle-Zinn "fragments" that are supposed to have agglomerated into the larger galaxies that we see today. If left in isolation, such an object may evolve into a dwarf galaxy with a small retinue of clusters. The GCSs in dE galaxies should then be similar in mass distribution (although not necessarily in metallicity) to those in giant galaxies. But, to date, no dwarf GCS has been studied that is populous enough to provide a very stringent test of this prediction.

Despite the small numbers of globular clusters that reside in dwarf galaxies, there are actually some practical advan-

[1] Visiting Astronomer, Cerro Tololo Inter-American Observatory (CTIO), National Optical Astronomy Observatories, which is operated by the Association of Universities for Research in Astronomy, Inc. (AURA), under cooperative agreement with the National Science Foundation.

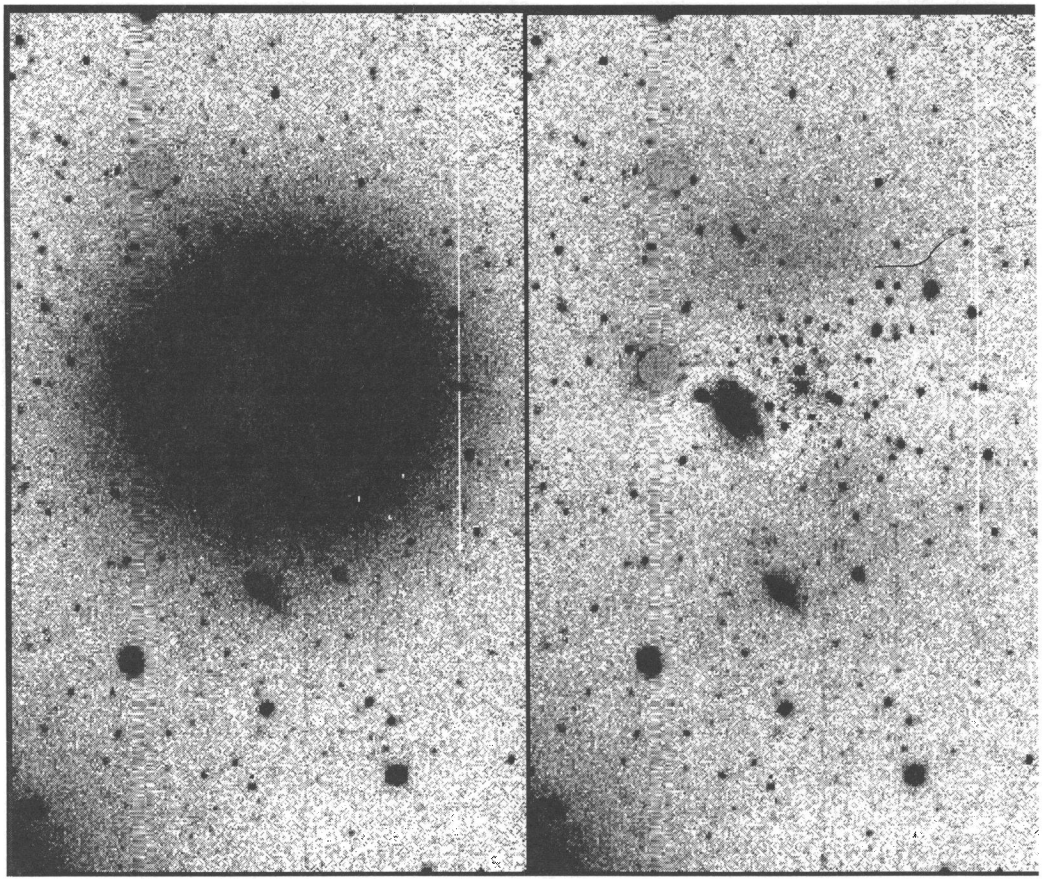

FIG. 1.—Combined *B* image of NGC 3115 DW1 with two saturated stars removed (*left*) and with the galaxy removed as described in the text (*right*). East is toward the top of the image, and north is to the right.

tages to studying them: because dE's mostly have low surface brightnesses, clusters can readily be detected by CCD imaging all the way into their centers. Also, their small spatial extent allows the *entire* GCS to be taken in easily, along with background, within a single CCD field.

In this paper we describe the first results of a more systematic survey of GCSs in dwarf galaxies. Data for 11 Virgo Cluster dE's, forming the major part of this work, will be presented in a second paper (Durrell, Harris, & Geisler 1996). Here we outline our methodology and discuss the results for the first target in our survey, the dE1,N galaxy near the large, edge-on S0 NGC 3115. NGC 3115 in turn is quite isolated (Tully 1982 places it in the extremely sparse and widespread Leo Minor group). Adopting the nomenclature of Caldwell (1983), we refer to the dwarf as NGC 3115 DW1; it is located 17′ from NGC 3115. This small galaxy was found to possess a very noticeable GCS by Hanes & Harris (1986). Because it is relatively nearby, isolated, and one of the brightest examples of a dE galaxy (see the discussion to follow), it presents an excellent first target for an analysis of a GCS in a dwarf elliptical.

2. OBSERVATIONS

BV images of NGC 3115 DW1 (MCG −1-26-21; $\alpha_{1950} = 10^h03^m12^s$, $\delta_{1950} = -7°44'14''$) were obtained on the nights 1985 December 10–12, at the prime focus of the CTIO 4 m telescope with the RCA1 CCD camera. This was the same observing run as described in the study of the Fornax cD galaxy NGC 1399 by Bridges, Hanes, & Harris (1991). The dE was imaged as a secondary target as time permitted during the run; in total, we obtained a single 900 s exposure in *V* and a 2 × 900 s pair in *B*. The usable field of the CCD had dimensions of 3′ × 5′ (300 × 508 pixels, with a scale 0.″6 pixel^{-1}). The galaxy nucleus was located near the center of the frame. The FWHM of the stellar images on both the *B* and *V* images was 1.″6.

The raw frames were preprocessed through standard bias-level subtraction and flat-fielding with dome flat exposures. The two *B* images were reregistered and co-added. Cosmic rays were removed with the "cosmic ray" package in IRAF[2], and two sets of columns affected by charge bleeding (and the two saturated stars that created them) were interpolated over with "fixpix"; otherwise, the frames were cosmetically excellent. Figure 1*a* shows the composite *B* frame after the above corrections were applied.

Calibration was carried out as described more completely in Bridges et al. (1991) from observations of Landolt (1983, 1992) and Graham (1982) standard stars on all 3 nights of the observing run. The expected random uncertainties in the photometry due to the calibration equations alone are $\sim \pm 0.015$ in *V* and ± 0.03 in *B*.

3. DATA REDUCTION

The GCS appears as a clustering of faint, starlike objects around the galaxy center. We first removed all the light from the galaxy itself by fitting elliptical isophotes to the

[2] IRAF is distributed by the National Optical Astronomy Observatories, which are operated by the Association of Universities for Research in Astronomy, Inc., under contract to the National Science Foundation.

galaxy, creating a smooth model and subtracting this from the images, with the STSDAS ellipse-fitting package in IRAF. For the isophote fits (which employed the method from Jedrzejewski 1987), we let the isophote center vary (although this has no effect on the profiles within the measurement uncertainties) and removed the brightest 20% of pixels in each isophote. The galaxy light profile was interpolated out to large enough distances to merge with the background sky, leaving no artifacts from the subtraction. This yielded a final, galaxy-subtracted image (an example of which is shown in Fig. 1*b*) for each filter. The innermost region ($r < 5$ pixels), with its steep brightness gradient, was the only unusable area of the frame. The results from the surface photometry of the dwarf are discussed briefly in the Appendix.

Inspection of the subtracted image clearly shows an excess of starlike objects surrounding the dwarf. DAOPHOT II (Stetson, Davis, & Crabtree 1990; Stetson 1992) was used to perform photometry of all objects on each frame. One pass of FIND (3 σ threshold) + PHOT + ALLSTAR was carried out; a second pass of DAOPHOT did not reveal any further objects and was therefore not used. Three bright, uncrowded stars were used to derive the point-spread function (PSF) for each image.

All globular clusters will appear as starlike images at the $\sim$11 Mpc distance (see § 6) of the galaxy at any ground-based resolution, so special attention was paid to purging as many as possible of the obviously nonstellar objects (background galaxies or badly blended images) from the photometry list through image classification (cf. McLaughlin, Harris, & Hanes 1994; Harris et al. 1991). Three parameters were used to remove such objects: (1) the DAOPHOT χ parameter, (2) the r_{-2} moment (Kron 1980), and (3) $\Delta M = M - m_{\rm ap}$, where $m_{\rm ap}$ is the (uncalibrated) aperture magnitude out to a radius of 3 pixels. Our culling limits for each parameter were then determined. In addition, any objects that lay within 5 pixels of the nucleus and within $\sim$14 pixels from the center of the background spiral galaxy (see Fig. 1) were also flagged and deleted. In the end, 13% of the measured objects were rejected as nonstellar.

Figure 2 shows the color-magnitude diagram (CMD) for all objects on the subtracted frame after application of the culling criteria described above. As will be seen below, most ($\sim$80%) of the objects in this diagram are either foreground stars or unresolved background galaxies; it is only within the inner $\sim 1'$ that the GCS dominates.

Artificial-star simulations were carried out in order to determine the photometric incompleteness of the data, the expected random photometric errors, and limits for the image classification procedure described above. We added 60 sets of 450 artificial stars each to the frames, following a luminosity function similar to that of the original data ($\sim$400 background stars and 50 artificial "globulars" with an r^{-2} distribution around the nucleus; see § 4 below). Each pair of images was reduced, and the detected stars matched in B and V just as the originals had been.

Figure 3 shows the r_{-2} values as a function of ΔV and ΔB for *all* the recovered artificial stars. The stellar sequence is obvious, and the dashed lines indicate the rejection boundary lines we have adopted ($r_{-2} \leq 1.40$ and ΔB and $\Delta V \leq 5.80$). Using these values (and applying DAOPHOT $\chi < 2.0$ for *both* filters), we found a total of 3.5% of the stellar objects to be misclassified as nonstellar. This effect is corrected for in the completeness function derived below.

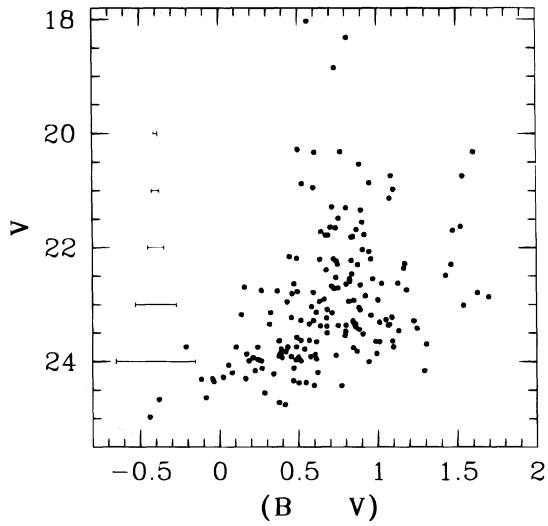

FIG. 2.—CMD for all objects in the figure that satisfied our classification criteria as described in the text. The error bars are the average random errors as determined from artificial star experiments.

This fraction increased to $\sim$7% within 80 pixels of the center, since the increased noise near the center of the galaxy makes some stellar objects appear artificially diffuse. Although still a small effect, this is also corrected for in the completeness tests.

Because of the radial dependence of the noise and the degree of crowding, we calculated the completeness function $f(V)$ for different annuli (width 25 pixels) surrounding the nucleus. Here we define f as the number of artificial stars added to a given magnitude bin that were recovered (regardless of where the star ended up) in *both* the B and V frames. The run of f versus magnitude was modeled by Pritchet's interpolation function (see Fleming et al. 1995):

$$f(V) = \frac{1}{2}\left[1 - \frac{\alpha(V - V_{\rm lim})}{\sqrt{1 + \alpha^2(V - V_{\rm lim})^2}}\right].$$

Here $V_{\rm lim}$ is the limiting magnitude in the sense defined by Harris (1990), as the magnitude where $f = 0.5$, and α is a parameter that measures how steeply f declines from 1 to 0. For all of the artificial star data in each annulus, we have determined α and $V_{\rm lim}$ using a maximum likelihood (M-L) technique that does not bin the data (cf. McLaughlin et al. 1994, 1995); the results are listed in Table 1. Note that the limiting magnitude is brighter (by about 0.5 mag) nearest the galaxy center due to the increased noise level. However, $V_{\rm lim} \sim 24.0$ for most of the frame. Using the same technique,

TABLE 1

PHOTOMETRIC COMPLETENESS

Radius	$V_{\rm lim}$	α	$N_{\rm add}$
3″–15″	23.406	0.8267	1260
15 –30	23.628	0.9826	1664
30 –45	23.880	1.8276	1936
45 –60	23.907	2.1957	2514
60 –75	23.922	2.2671	3026
75 –90	23.944	2.5951	3409
90 –105	23.976	2.4387	3316
105 –120	23.933	2.2701	2737
120 –135	23.992	2.7631	2635
135 –150	23.859	1.7792	1965
150 –165	23.959	2.1520	1345
165 –195	23.905	2.1443	972

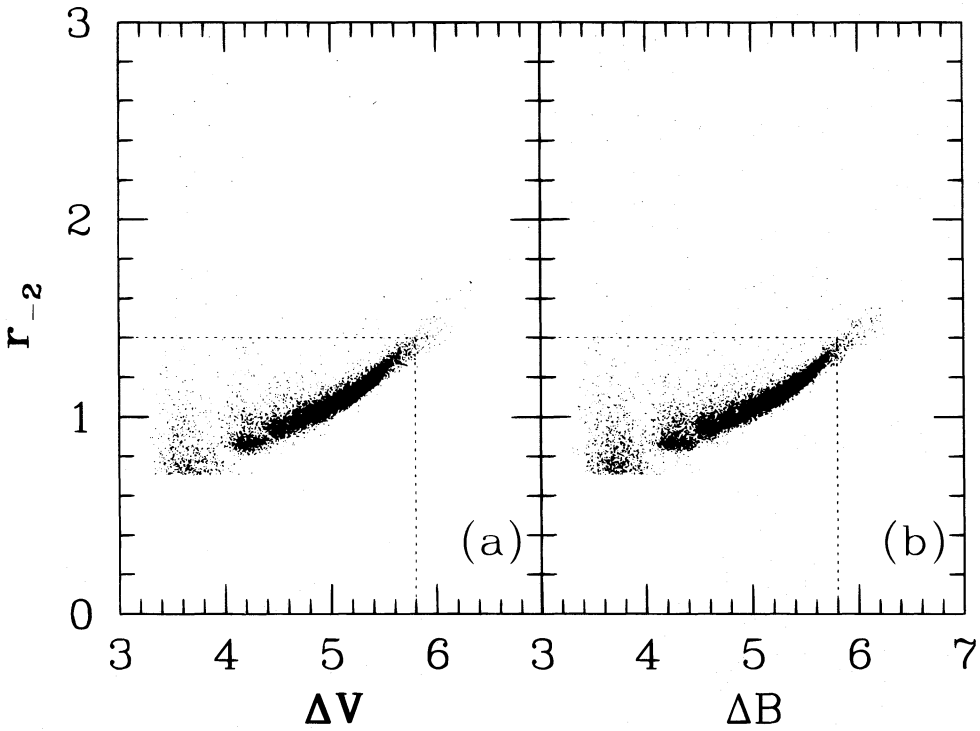

FIG. 3.—Image classification diagram for artificial stars. The r_{-2} central concentration moment is plotted against Δm, the difference between the PSF-fitted and aperture magnitudes. The dotted lines indicate the adopted boundaries for stellar objects: $r_{-2} < 1.4$, and ΔV and $\Delta B < 5.8$.

we find $B_{\rm lim} \sim 24.8$ for most of the frame (but with $B_{\rm lim} \sim 24.2$ in the innermost annulus).

The random photometric errors were also determined from the artificial star experiments, and the 1 σ errors are plotted in Figure 2. Brighter than the limiting magnitude ($V \sim 24$), there are no significant systematic color shifts, and the random errors in each bandpass are less than 0.25 mag.

4. RADIAL DISTRIBUTION

The extent and radial profile of the GCS were determined by counting the stellar objects in a series of circular annuli about the galaxy center, out to the edge of the frame. For n stars observed in a given annulus j, the *true* number of objects is $N(j) = \sum_{i=1}^{n} f(V_i)^{-1}$. The uncertainty in $N(j)$ is simply $n^{1/2}$ divided by $f_{\rm eff} = n/N(j)$.

All objects with $V \leq 23.75$ that passed the image classification criteria were used to derive the radial distribution of the GCS (Table 2 and Fig. 4). In Table 2, the radius r is the mean radius for all objects located in a given annulus, and the area (given in square arcminutes) is that actually present on the frame. There is a clear excess in the surface density σ for $r < 48''$ (the central area of 2 arcmin^2), beyond which σ is nearly uniform. To derive a background level, we have computed σ for five regions around the outer parts of the frame having the same area as that of the central GCS, yielding $\sigma_{\rm bkg} = 6.4 \pm 1.9$, where the error is simply the rms scatter about the mean value. This estimate realistically includes any scatter due to background galaxy "clumps" as well as the normal $n^{1/2}$ statistics. The final two columns of Table 2 list the residual surface density $\sigma_{\rm cl} = \sigma - \sigma_{\rm bkg}$, presumed to be due to the globular clusters around NGC 3115 DW1.

From the $\sigma_{\rm cl}$ values given in Table 2, we derive a total number of 39 ± 8 clusters for $r < 48''$ (equivalent to $r < 2.5$ kpc for an adopted distance $d \sim 11$ Mpc); after correcting for the presence of the background spiral galaxy, we derive a total population of $N = 41 \pm 8$ clusters for $V \leq 23.75$. We will defer further discussion of the specific frequency to § 7.

It is of interest to determine how the radial profile of the GCS compares with that of the galaxy light itself; in most *large* ellipticals, the GCS is more extended than the halo light (Harris 1986, 1991a). Figure 5 is a log-log plot of surface density versus radius for both the cluster system and the B surface brightness profile. To within the observational uncertainties, the cluster distribution appears to follow the galaxy light, although a profile shallower than the galaxy light is also consistent with the data. A least-squares fit to

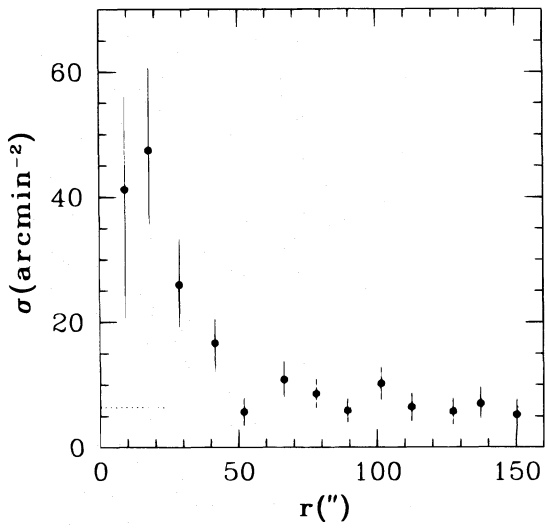

FIG. 4.—Radial profile (corrected for incompleteness) of all objects on the frame with $V < 23.75$. Here σ is the number per square arcminute. The dotted line shows the background level.

TABLE 2

RADIAL PROFILE (V < 23.75)

r	N	$\epsilon(N)$	Area[a]	σ	ϵ	σ_{cl}	ϵ
9″.3.....	4.8	2.4	0.116	41.2	20.6	34.8	20.7
18.0.....	16.9	4.7	0.355	47.5	13.2	41.1	13.3
28.8.....	15.5	4.5	0.596	26.0	7.5	19.6	7.7
41.5.....	14.5	4.0	0.868	16.7	4.6	10.3	4.9
51.9.....	6.2	2.5	1.091	5.7	2.3	−0.7	2.9
66.5.....	15.0	4.0	1.382	10.8	2.9	4.4	3.4
78.2.....	15.4	4.1	1.624	8.6	2.5	2.2	3.0
89.3.....	9.6	3.2	1.639	5.9	2.0	−0.5	2.7
101.4.....	15.3	4.1	1.501	10.2	2.7	3.8	3.2
112.5.....	9.0	3.2	1.390	6.4	2.3	0.0	2.9
127.4.....	7.7	2.9	1.342	5.8	2.2	−0.6	3.0
137.2.....	7.6	2.9	1.081	7.0	2.7	0.6	3.2
150.2.....	4.2	2.1	0.809	5.2	2.6	−1.4	3.2

[a] Area in square arcminutes.

the three points within $1.1 < \log(r) < 1.7$ gives $\sigma_{cl} \propto r^{-1.64\pm0.80}$.

Of note is the apparent flattening of the cluster density profile within 20″ (~1 kpc) of the nucleus. This feature was noted by Hanes & Harris (1986) on the basis of photographic star counts and is confirmed here with the ability of CCD imaging to reveal the GCS population right into the galaxy nucleus, and the added security of quantitative incompleteness tests. However, we note that the large uncertainties on σ_{cl} (only four objects are observed in the innermost annulus) do not allow us to distinguish whether the observed trend is a simple flattening of the cluster distribution or a *drop* in σ_{cl}, i.e., an actual depletion of globular clusters in the inner 1 kpc. For example, if a large fraction of the "original" globular clusters have been disrupted, then one might speculate that the nucleus of the nucleated dwarf is made up of former globulars. There are, however, a couple of reasons why this idea is unlikely to be true. First, the nucleus is redder [by ~0.15 in $(B-V)$ in the mean; see the Appendix] than most of the globular clusters, which would require the nucleus to have formed preferentially from very metal rich objects (see similar arguments for M31 by van den Bergh 1991 or Surdin & Charikov 1977). This is improbable, particularly in a dwarf galaxy where most clusters are generally metal poor, and where there is no apparent metallicity gradient. Second, there is a problem of sheer numbers of required clusters; many dozens of them would have been needed to form a system as luminous as the nucleus we now see. Assuming $M/L \sim 3$ (Peterson & Caldwell 1993) and $M_V \sim -12.8$ for the nucleus (see the Appendix), we derive a mass of $\sim 3 \times 10^7\ M_\odot$, more than 200 times more massive than an "average" globular. Alternative, more plausible, models for forming a compact nucleus are discussed by Freeman (1993).

If the radial distribution of the GCS is more nearly primordial and not due to globular cluster disruption, then our omission of the innermost point in the power-law fit may be invalid. If we choose instead to do a King-model fit to Figure 5, we derive an approximate core radius of the GCS of ~27″, which is twice as large as that of the galaxy light (~14″.5; see the Appendix). That is, the inner GCS is notably *less* concentrated than the galaxy light. This same effect is discussed extensively for the cD galaxy M87 by McLaughlin (1995), who concluded that the much larger core radius of the GCS in M87 is primordial in origin, and not the result of dynamical friction or GC destruction processes.

4.1. *Spatial Distribution*

The spatial distribution of all stellar objects on the frame is plotted in Figure 6. Of interest is the slight asymmetry of objects near the nucleus; within our 48″ central circle, there are 18 objects north of the nucleus and 12 to the south (after subtraction of a uniform background population). Within Poisson statistics, these numbers, however, are consistent with a uniform distribution of clusters about the nucleus. The probability that a galaxy cluster would be located by chance so close to the nuclear region of the dwarf is a priori very small; roughly 10 such clusters are seen per square

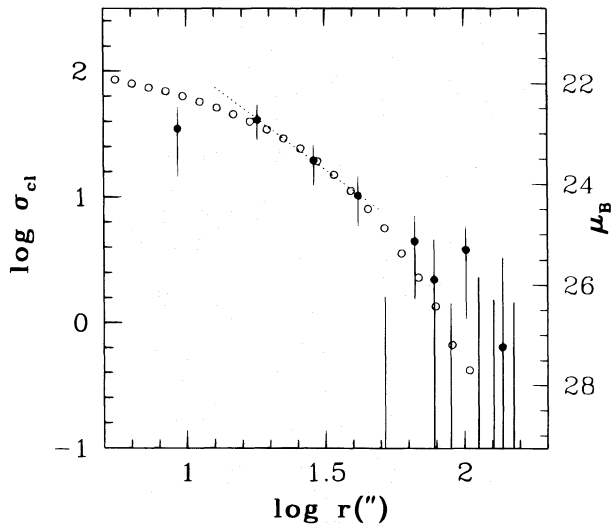

FIG. 5.—Background-subtracted radial profile of the NGC 3115 DW1 GCS (*filled circles*) superimposed on the *B* surface brightness profile (*open circles*). An arbitrary vertical shift has been applied to match the profiles. The dotted line has a slope −1.64 (see § 4 of the text).

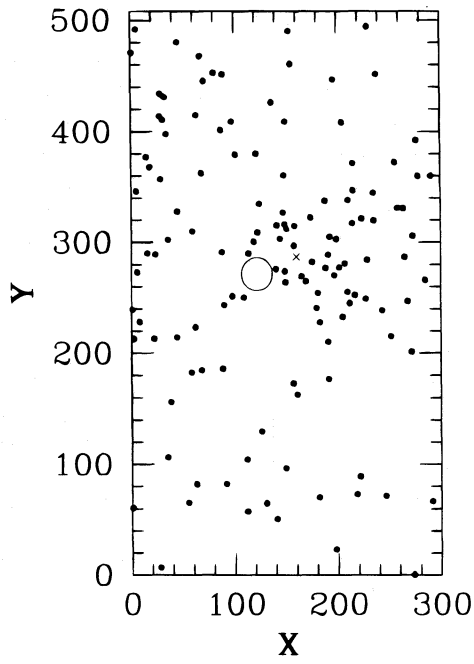

FIG. 6.—Spatial distribution of all objects (with $V \leq 23.75$) on both frames that pass the image classification criteria. The cross denotes the galaxy nucleus, and the large open circle that of the position of the background galaxy.

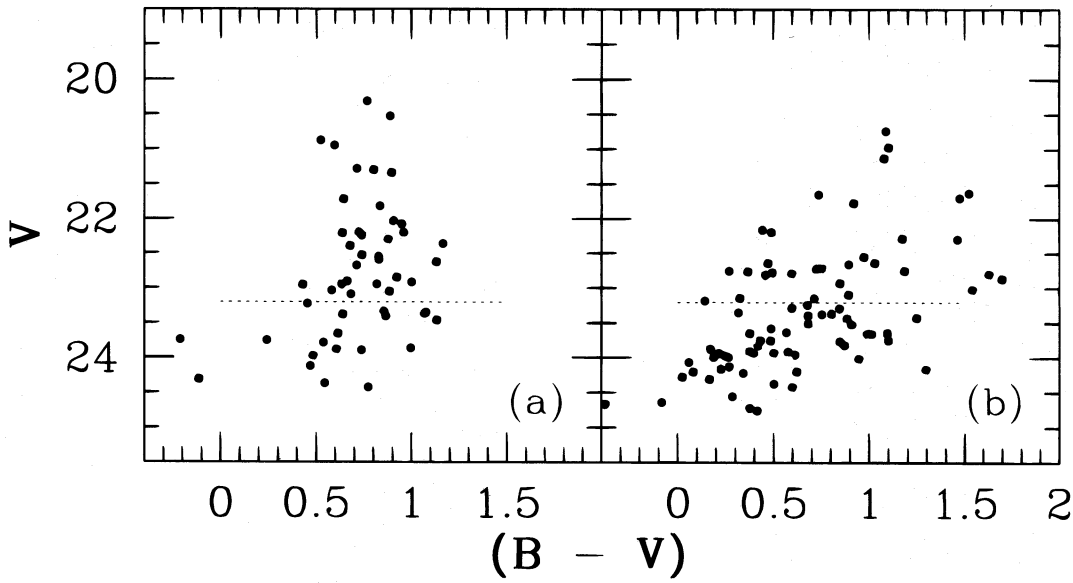

FIG. 7.—CMDs for all objects with (*a*) $r < 80$ pixels ($=48''$) and (*b*) $r > 140$ pixels ($=84''$). The dotted lines indicate the faint cutoff as mentioned in the text.

degree in background fields taken by J. Secker (1995, private communication). Thus, the likelihood that the center of a galaxy cluster would lie within 30″ of the dE nucleus is less than 0.5%; furthermore, the cluster would have to be located in a constrained range in distance so that the brightest cluster members have $V \sim 21$. Inspection of the Canada-France-Hawaii Telescope I images of this galaxy (kindly provided by J. J. Kavelaars), with slightly better seeing (1.″3) than our images, shows that only one of our stellar objects within 80 pixels of the nucleus appears to be nonstellar. Given this, we conclude that most of the observed excess is due to a GCS.

5. GLOBULAR CLUSTER SYSTEM METALLICITY

We can use the observed colors of the NGC 3115 DW1 GCS to estimate the chemical composition of the constituent clusters. Although $(B-V)$ is not strongly sensitive to metallicity, it is still useful to determine the *mean* metallicity of the GCS and to search for any global trends.

To define a sample of "pure" globular clusters from our sample, we now consider only those objects within 48″ of the galaxy center (see Fig. 7*a*) and with $V < 23.2$, so that incompleteness in B does not introduce an unwanted color bias in our results. The remaining objects in the figure (Fig. 7*b*) then define the background sample (note the much greater scatter in this plot). We have statistically removed (by matching objects in both samples with similar locations in the CMD, normalized to the same area) four "background" objects from the $r < 48''$ sample, thus leaving a statistically "clean" globular cluster sample of 24 objects.

The mean color of these objects is $(B-V) = 0.763 \pm 0.026$. For the foreground reddening—fortunately quite small, since the NGC 3115 field is at high latitude—we assume $E(B-V) = 0.025$ ($A_V = 0.08$) from Burstein & Heiles (1984). Correcting for this, we then derive $(B-V)_0 = 0.74 \pm 0.03$. To convert to metallicity, we use $(B-V)_0 = 0.200[\mathrm{Fe/H}] + 0.971$ from the calibration of Couture, Harris, & Allwright (1990), yielding a mean metallicity $\langle[\mathrm{Fe/H}]\rangle = -1.16 \pm 0.13$ for the GCS. However, given the photometric scatter ($\sigma \sim 0.05$ for $V = 22$) and possible zero-point uncertainty ($\sigma \sim 0.03$), the true (external) uncertainty in the mean metallicity could be as large as ~ 0.3 dex. There is also no apparent color gradient in the GCS (Fig. 8). A formal fit to the data reveals $\Delta(B-V)/\Delta \log(r) = 0.2 \pm 0.2$.

Although it is not well resolved by our photometry, there does appear to be a significant cluster-to-cluster dispersion in intrinsic color (and thus, by assumption, in metallicity). Inspection of Figure 7*a* shows that the color scatter is present even at the brighter magnitudes where the photometric uncertainties are negligible; the observed dispersion of $\sigma_{B-V} \simeq 0.13$ corresponds to $\sigma_{[\mathrm{Fe/H}]} \simeq 0.6$ dex. By comparison, for the Milky Way halo clusters (e.g., Zinn 1985), the mean metallicity is $\overline{[\mathrm{Fe/H}]} \simeq -1.6$, and the rms dispersion is $\sigma_{[\mathrm{Fe/H}]} \simeq 0.3$. Our data therefore suggest that even though NGC 3115 DW1 is a relatively small galaxy—and has only about one-third as many globular clusters as the entire Milky Way—the GCS is 2–3 times more enriched in chemical composition and has a higher internal metallicity dispersion as well.

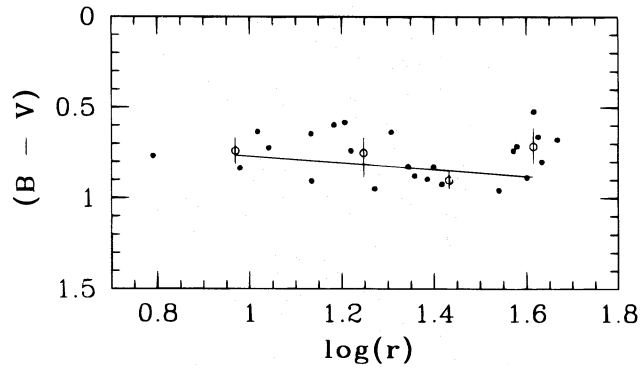

FIG. 8.—Color gradient of the GCS. The filled circles represent the original data (the "cleaned" GC sample), and the open circles are the average binned colors. The straight line denotes the best fit to the four points.

The color of the galaxy light in the region occupied by the GCS is $(B-V)_0 \sim 0.91 \pm 0.04$ (see the Appendix), so the globular clusters are indeed bluer (and, by inference, more metal poor) than the halo light by 0.17 mag in the mean. We have adopted [Fe/H] $\simeq -0.7$ for the galaxy light (see the Appendix), so the GCS is on average about 0.5 dex more metal poor than the galaxy. This is remarkably similar to the metallicity offset between GCS and halo light that has been found for many large E galaxies (Harris 1991a; Ajhar, Blakeslee, & Tonry 1994), and in other dE galaxies as well (Harris 1983; Da Costa & Mould 1988). The normal interpretation of this offset is that the globular clusters formed before the rest of the galaxy and may indeed have been responsible for seeding the enrichment of the halo stars (see the references cited, as well as De Young, Lind, & Strom 1983; HP94).

Our derived metallicity for the GCS in NGC 3115 DW1 adds scatter to, but is consistent with, the conventional relation between [Fe/H] and galaxy luminosity (Brodie & Huchra 1991; Harris 1991a; Zepf, Ashman, & Geisler 1995). For only a dwarf galaxy, it has a surprisingly high GCS metallicity level, being comparable (for example) to the mean [Fe/H] for the GCS of M31, a much more massive galaxy, and not too far below the [Fe/H] ~ -1 level that is characteristic of giant ellipticals (Harris 1991a). The most recent calibration of the [Fe/H] versus luminosity relation (Secker et al. 1995) indicates that a mean metallicity of ~ -1.5 would nominally be expected for the NGC 3115 DW1 GCS, although we stress that such a value is barely allowed within our observational errors.

It is interesting that within the errors, the nucleus (see the Appendix) is as red as the reddest globular clusters, and this may be a hint as to how the dwarf evolved. This dwarf may prove to be an excellent probe of dwarf galaxy evolution since it seems likely to have been little affected by subsequent interactions and mergers. The existence of a luminosity-metallicity relation for dwarfs (Caldwell et al. 1992; Da Costa 1992) has been considered evidence for supernova-driven winds dominating the evolution of dwarfs (Yoshii & Arimoto 1987; Dekel & Silk 1986; Vader 1986); the more massive dwarfs are more able to keep their gas (and enrich it further) before final expulsion. The rather surprisingly high metallicity of the globular clusters in NGC 3115 DW1, and of the galaxy itself, fits this general trend.

6. THE GLOBULAR CLUSTER LUMINOSITY FUNCTION AND THE DISTANCE TO NGC 3115 DW1

The globular cluster luminosity function (GCLF) $\phi(V)$ has been determined by binning all objects in the globular cluster sample (Fig. 7*a*) in 0.5 mag bins and by counting objects in the same manner as for the radial distribution. The background luminosity function comprises all objects in the control sample and scaled to match the area covered by the globular cluster sample. The results are listed in Table 3 and plotted in Figure 9. Although the uncertainties are large, there is an indication that the turnover has been reached.

We fitted the observed $\phi(V)$ with a t_5 distribution, which has been found to describe other GCLFs somewhat better than the traditional Gaussian (Secker 1992; Secker & Harris 1993; Harris, Harris, & McLaughlin 1995). To do this, we first estimate the dispersion σ_{t5}. Given the power-law slope γ of the GCS *mass function* (below), the appropriate *Gaussian* dispersion is $\sigma_G \simeq 1.30\,|1+\gamma|^{-1}$ (McLaughlin 1994); but from Secker (1992), we also have $\sigma_G \simeq 1.29\sigma_{t5}$, so that $\sigma_{t5} \simeq |1+\gamma|^{-1}$. Thus, with $\gamma = -1.8 \pm 0.4$ (see below), $\sigma_{t5} = 1.2 \pm 0.6$. This parameter was therefore fixed at 0.6, 1.2 (best fit), and 1.8, resulting in a fitted turnover, or peak, magnitude of $V_{TO} = 23.1^{+0.8}_{-0.5}$ for the NGC 3115 DW1 GCS. These three t_5 fits are drawn in Figure 9, along with a scaled version of the M87 GCLF from Harris et al. (1995). Evidently, our error estimates are quite liberal, since the fits with $\sigma_{t5} = 0.6$ or 1.8 are noticeably poorer than that for $\sigma_{t5} = 1.2$.

The luminosity of the GCLF turnover can be used as a distance indicator, as discussed at length by Jacoby et al. (1991) and Harris (1991a). To do this, we have assumed the absolute magnitude of the GCLF turnover to be $M_{V,TO} = -7.17 \pm 0.09$, as determined by Fleming et al. (1995) from the GCLFs for nine *large* elliptical galaxies. This calibration is based primarily on an adopted Virgo distance modulus of $(m-M)_0 = 31.0$ (Jacoby et al. 1992; Pierce et al. 1994; Freedman et al. 1994). Although it is not clear a priori whether we should be comparing the GCLF in this dwarf E

TABLE 3

GLOBULAR CLUSTER LUMINOSITY FUNCTION

V	N_{obs}[a]	ϵ	N_{bkg}[b]	ϵ	N_{cl}	ϵ
20.5.....	2.04	1.44	0.22	0.22	1.82	1.46
21.0.....	2.04	1.44	0.43	0.30	1.61	1.47
21.5.....	4.17	2.09	0.65	0.37	3.52	2.12
22.0.....	7.67	2.90	0.65	0.38	7.02	2.92
22.5.....	8.96	3.17	1.98	0.66	6.98	3.24
23.0.....	12.65	4.00	3.35	0.86	9.31	4.09
23.5.....	14.03	4.68	4.86	1.12	9.17	4.81
24.0.....	16.54	6.75	10.92	2.38	5.62	7.16

[a] Number of objects observed per 0.5 mag bin ($r < 48''$).
[b] Scaled number of background objects per 0.5 mag bin ($r > 84''$).

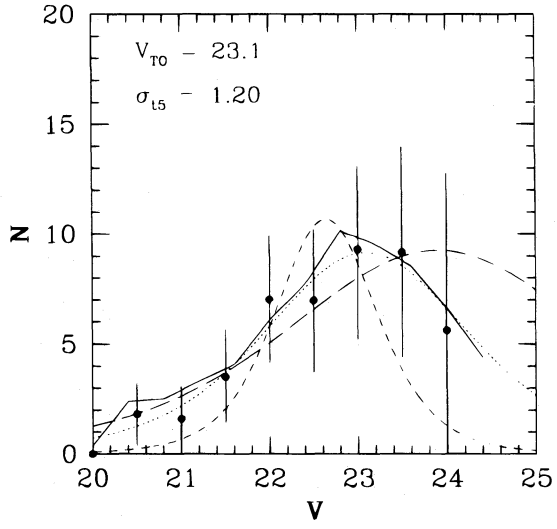

FIG. 9.—Incompleteness-corrected GCLF for NGC 3115 DW1. The dotted line is the best-fit t_5 function, with the given parameters. The solid line is the M87 GCLF from Harris et al. (1995), which has been shifted 0.5 mag brighter to adjust for the nearer distance of NGC 3115 ($V_{TO,M87} = 23.55$) and scaled down by a factor of 11 to account for the much smaller total GCS population in the dwarf. The dashed lines show the best fits assuming fixed values of $\sigma_t = 0.6$ (medium dashed line) and 1.8 (large dashed line).

galaxy with those in giant E galaxies or spiral galaxies, or neither, we note that (1) in practice, the GCLF turnover luminosity in spirals (Fleming et al.) is scarcely brighter, at $M_{V,\mathrm{TO}} \simeq -7.4$, and (2) the observed mean luminosities of the globular clusters in the Local Group dwarf ellipticals are not *significantly* different from either the spirals or the gE's (Harris 1991a), although the small number of globulars in the former makes this point less certain. From our derived value of V_{TO}, we then derive $(m - M)_V = 30.3^{+0.8}_{-0.5}$ for the dwarf. With $A_V = 0.08$, our deduced distance to NGC 3115 DW1 is $11^{+5}_{-2.3}$ Mpc.

There have been no previous estimates of the distance to the dwarf galaxy itself, although we can compare it with distances for NGC 3115. From an early study of its GCLF, Hanes & Harris (1986) derived a distance range of 8–12 Mpc. Ciardullo, Jacoby, & Tonry (1993) quote distances based on both the surface brightness fluctuation method [SBF; $(m - M)_{0,\mathrm{SBF}} = 29.65 \pm 0.25$] and the planetary nebulae luminosity function [PNLF; $(m - M)_{0,\mathrm{PN}} = 30.17 \pm 0.13$]. Our result is in excellent agreement with the PNLF result and marginally consistent with the SBF result, although Ciardullo et al. (1993) do note possible problems with the SBF value. As noted in the Appendix, this distance is not in agreement with that expected ($\sim$4 Mpc) from the M_B-n relation of Young & Currie (1994), which is widely discrepant.

Although the distance to NGC 3115 DW1 therefore seems quite similar to that for NGC 3115, can we then assume that the dwarf is actually a companion of the much larger S0? At a distance of 11 Mpc, their projected separation of 17′ translates to $\sim$55 kpc, not unusual for dwarf/giant pairs in a loose group (Vader & Chaboyer 1994). The heliocentric radial velocities for the S0 and the dE, N are also similar: 670 km s^{-1} (RC3; de Vaucouleurs et al. 1991) and $\sim$720 km s^{-1} (Peterson & Caldwell 1993), respectively. Binggeli, Tarenghi, & Sandage (1990) argue that true *field* dE's are very rare, and *nucleated dwarfs* are only found in galaxy clusters or near large galaxies (Ferguson & Binggeli 1994). We conclude that the dwarf galaxy is most likely a true physical companion of NGC 3115.

The *mass spectrum* of the GCS has been derived from the GCLF from the prescription given in McLaughlin et al. (1995) (see also McLaughlin 1994):

$$N(L_V) \simeq 2.5\phi(M_V)(\delta \ln 10)^{-1} 10^{0.4(M_V - M_{V,\odot})} ,$$

where $\delta = 0.5$ is the magnitude bin width and $N(L_V)$ is the number of clusters per unit luminosity [$N(L_V)$ is directly equivalent to the *mass* distribution function $N(m)$ if M/L is constant]. The results are plotted in Figure 10, which clearly shows the power-law behavior discussed by HP94, $N(L_V) \sim L_V^{\gamma}$. As discussed at length by McLaughlin (1994), the slope γ of the mass spectrum changes at the GCLF turnover, which is the peak point in the graph of cluster numbers per unit *magnitude*. Although our data reach only slightly fainter than the turnover, it is evident here as a flattening of γ in the $N(L_V)$-plane. Fitting a single power-law curve to all but the two faintest points, we find $\gamma = -1.8 \pm 0.4$, as shown in Figure 10.

This mass-spectrum slope, the first derived for a dwarf galaxy, is encouragingly compatible with those found over a similar range of globular cluster masses in many larger galaxies of widely different sizes and morphologies (HP94). The processes of dynamical destruction of clusters (due to the full array of bulge shocking, disk shocking, dynamical friction, and cluster evaporation coupled to the parent galaxy's tidal field) must have very different amplitudes in all of these diverse galaxies, and we find it highly improbable that such remarkably similar cluster mass distributions can have resulted from convergent evolution starting from widely different initial GCLFs. Following HP94 and McLaughlin & Pudritz (1996), we suggest instead that the significance of the mass-spectrum data is that *the mechanism of globular cluster formation was the same in all types of galaxies*, from dwarfs ($M \sim 10^9\ M_\odot$) to the giant cDs ($M \sim 10^{13}\ M_\odot$). This idea is developed further in McLaughlin & Pudritz (1996).

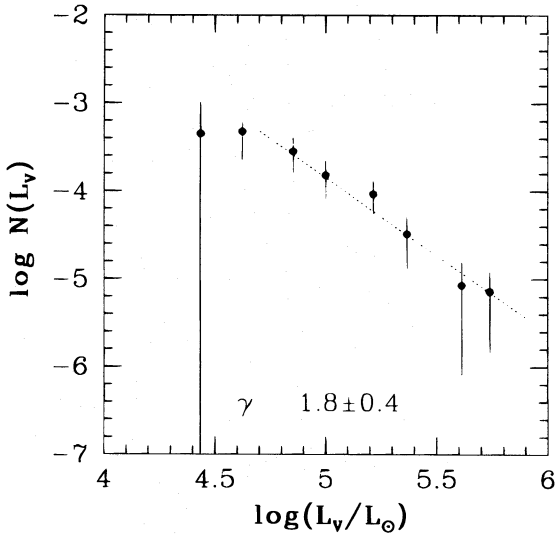

FIG. 10.—Mass (luminosity) spectrum of the GCS. The number of clusters per unit *linear* luminosity, $N(L_V)$, is plotted against L_V. The solid line is the best fit of the power-law model $N \sim L^{\gamma}$ to all points except the faintest two points. Note that the shallowness of N at low masses [$\log(L_V) < 4.7$] is real and is responsible for the GCLF turnover.

7. SPECIFIC FREQUENCY

The fraction of the GCLF brighter than $V = 23.75$ was found by integrating over the best t_5 fit, yielding 0.70 ± 0.14. The uncertainty in this value was derived by adopting errors of 0.3 mag in V_{TO} (from arguments in the previous section, we can constrain the distance error to be similar to that for NGC 3115) and 0.4 in σ_{t_5} (again, smaller than the error derived in the previous section, for reasons mentioned there). The *total* number of clusters in the GCS is then 59 ± 23. With $M_V = -17.7$ for the galaxy (see the Appendix), the specific frequency (number of globulars per unit galaxy light; Harris & van den Bergh 1981) of the NGC 3115 DW1 GCS is $S_N = 4.9 \pm 1.9$. Of note is our value for $M_{V,T}$, since it is a full magnitude brighter than generally believed (Peterson & Caldwell 1993 list $M_V = -16.7$); the change is primarily due to the larger distance we have derived.

Hanes & Harris (1986) similarly found a specific frequency of 5 ± 2.5 for this dwarf, clearly larger than that of the "parent" galaxy NGC 3115, for which $S_N \sim 2 \pm 0.5$ if $d = 11$ Mpc. Our data reinforce their conclusion that globular cluster formation proceeded more efficiently in the dwarf than in the larger S0 galaxy and is in fact comparable to the giant ellipticals in Virgo and Fornax (where $S_N \approx 5$ on average; Harris 1991a). Interestingly, it appears that the efficiency of globular cluster formation was *generally* higher

in dE's than in late-type galaxies (as an example, the Local Group dE's have $S_N \sim 2$–7 [Harris 1991a], while most spirals have lower specific frequencies by factors of 3 or more). In Paper II (Durrell et al. 1996) we will considerably add to the evidence supporting this claim with data from several Virgo dE galaxies.

8. CONCLUSIONS

We have carried out a multicolor study of the GCS in the luminous dE,N galaxy NGC 3115 DW1, the first such study of a dwarf galaxy outside the Local Group. The GCS constitutes what appears to be a quite "normal" (by E galaxy standards) globular cluster population, with a specific frequency $S_N \simeq 5$ and a metallicity $[\mathrm{Fe/H}]_{B-V} \sim -1.2$. We suggest as well that the observed cluster-to-cluster dispersion in color represents a real internal metallicity dispersion of up to ~ 0.6 dex. As in giant E galaxies, the GCS is more metal poor than that of the stellar population in the dwarf galaxy halo by perhaps 0.5 dex. There is no significant metallicity gradient in either the galaxy or the GCS, and the radial profile of the GCS is similar to that of the galaxy light, outside of a core which is roughly a factor of 2 larger than that of the halo light.

The GCLF has been used to derive a distance modulus $(m - M)_V = 30.3^{+0.8}_{-0.5}$ for the dwarf. This is consistent with distance estimates for NGC 3115 itself, so the dwarf is likely a true companion of the S0 galaxy. The globular cluster mass spectrum has a power-law index of $\gamma = -1.8 \pm 0.4$, similar to those observed in giant galaxies. This is strong evidence that the mechanisms of globular cluster formation are fundamentally the same in most galaxies over a large range in galaxy mass. The specific frequency of the dwarf ($S_N = 5 \pm 2$) is 2–3 times as large as in NGC 3115 itself (or M31, or the Milky Way) and is consistent with that of the Local Group dE's.

Surface photometry of the dE,N galaxy, coupled with the revised distance modulus, shows that it is brighter than previously believed ($M_V \sim -17.7$) and is in fact among the most luminous examples of a dE galaxy. The nucleus is also luminous ($M_V \sim -13$) and has a color that is similar to that of the rest of the galaxy but much redder than its clusters. The inferred high metallicity of the galaxy and its GCS indicates that supernova-driven winds may have been important in the galaxy's evolution, and that the depletion of gas must have occurred at a sufficiently late time to allow metal enrichment of the many populations present in the galaxy.

The authors would like to thank Jeff Secker for helpful comments throughout the project, and Howard Bushouse for his technical assistance with STSDAS. The work presented here has been partially supported by NSERC Fellowships to P. R. D. and D. E. M, and operating grants to W. E. H. and D. A. H.

APPENDIX

SURFACE PHOTOMETRY OF NGC 3115 DW1

The surface brightness profile for the galaxy, in both B and V, is plotted in Figure 11. The errors are those supplied by ELLIPSE plus those introduced by the uncertainty in the sky level (about 1%) for each frame. The sky level was determined from a small region on each frame farthest from the galaxy center. This yielded a self-consistent solution, since the model for each galaxy, when properly extrapolated, reached the sky level well before the edge of the frame. The on-frame standards (see § 2) have been used to calibrate the surface photometry.

The surface brightness profile clearly shows the trademarks of a dE,N galaxy: an approximately exponential falloff along with a bright central excess (the nucleus). The profile is not well fitted by a single exponential $I = I_0 e^{-r/r_0}$ but closely resembles the profile type IIIb as defined by Binggeli & Cameron (1991; hereafter BC91). Such deviations from a single exponential fit appear to be common in bright dE's (Cellone, Forte, & Geisler 1994; Young & Currie 1994; Caldwell & Bothun 1987), and the most recent works have included a "shape" parameter n ($I = I_0 e^{-(r/r_0)^n}$). This modified-exponential

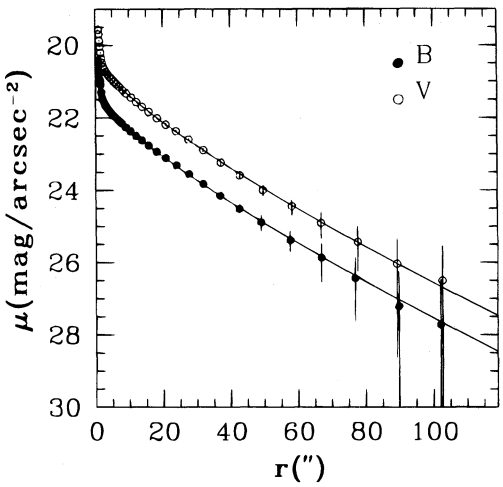

FIG. 11.—B and V surface brightness profiles as determined in the text. Here r is the average radius of the isophote. The solid lines represent the best-fit modified exponentials to the data (see text).

relation fits our profile very well with $n \sim 0.8$ (outside of 7″), particularly in the mid-to-outer regions of the galaxy (Fig. 11). A King (1966) model with a core radius $r_c = 14\farcs4$ (= 770 pc for $d = 11$ Mpc) and concentration index $c \sim 1.4$ also provides a very good fit to the data.

The total magnitudes for the galaxy were determined using the surface brightness profiles. Out to the final radius of the isophote fitting ($r = 104''$, $\mu_B \sim 27.7$, $\mu_V \sim 26.5$), the magnitudes are $V_T = 12.63 \pm 0.06$ and $B_T = 13.57 \pm 0.09$ (accounting for errors in calibration boosts the uncertainties to $\sim$0.1 mag). As a check on these values, we have compared our results with that of Caldwell (1983), who measured (photoelectrically) BV values for this galaxy with a 58″.6 aperture. From our photometry, we derive $V = 13.45 \pm 0.02$ and $(B-V) = 0.90 \pm 0.03$ for the same radius; these agree very well with $V = 13.45 \pm 0.01$ and $(B-V) = 0.87 \pm 0.01$ from Caldwell's study. However, the galaxy color is markedly different from the $(B-V) = 0.73$ listed in the RC3 (de Vaucouleurs et al. 1991).

Our adopted values for n and M_B (~ -16.8) lie quite far off the relation between these parameters as found by Young & Currie (1994). In their calibration, $n = 0.8$ corresponds to $M_B \sim -14.6$, which would imply a distance of $\sim$4 Mpc, clearly inconsistent with the value we have derived in § 6 above. The reason for this large discrepancy is unclear to us. There is the possibility that the shape of the NGC 3115 DW1 profile has changed over time, perhaps by some tidal trimming from NGC 3115 in the distant past (there is little evidence for any *recent* interaction). However, a rough estimate of the tidal radius of the dwarf, based on the closest passage of 50 kpc (its present projected separation), is $\sim$11 kpc, or $\sim$200″ at a distance of 11 Mpc, which is well beyond the outermost isophotes.

The profiles in both B and V are remarkably similar, and a simple subtraction of one from the other (Fig. 12) shows that there is little gradient in $(B-V)$ throughout the galaxy; a formal fit to the points between 5″ and 50″ (the range over which we observe most of the GCS) yields $\Delta(B-V)/\Delta \log (r) = -0.026 \pm 0.043$. This result is consistent with previous observations of dwarf galaxies, over half of which have no color gradient (Vader et al. 1988; Chaboyer 1994).

The mean color for $5'' < r < 50''$ is $(B-V) = 0.94 \pm 0.01$, with the error simply that of the mean points; the external uncertainty is dominated by the calibration zero-point errors and is likely to be at the 0.03–0.04 mag level. This color (dereddened) corresponds to [Fe/H] ~ -0.3 if we assume a "normal" old population (which is indeed the case for Local Group dE's; Lee, Freedman, & Madore 1993; Davidge 1994). However, this value is highly uncertain since the [Fe/H]-$(B-V)$ relation is poorly defined at such high metallicities (very few Milky Way globulars have such high metallicities, and none with well determined reddenings). Use of the luminosity-abundance relation for the dE's in the Local Group (Caldwell et al. 1992) predicts a value of $\sim -0.7 \pm 0.2$, and this relation has been extended to dE's in the Fornax cluster by Cellone et al. (1994). In addition, Brodie & Huchra (1991) derive [Fe/H] $= -0.99 \pm 0.58$ for NGC 3115 DW1 based on absorption line indices, although there is a wide range in [Fe/H] for their brightest dwarfs. We adopt a metallicity of ~ -0.7, although with an uncertainty of about 0.3 dex.

The position angle θ for each isophote as a function of radius is given in Figure 13 (*top*) and shows no twisting of the isophotes over most of the galaxy, consistent with little or no tidal disruption in the recent history of the dwarf. This is further supported by the lack of *any* significant deviation of the isophotes from an elliptical shape. The coefficients for the cos (3θ), sin (3θ), cos (4θ), and sin (4θ) terms are all consistent with zero (cf. Peletier et al. 1990). This result was not unexpected since the dwarf lies in a very sparse environment. There are some differences in θ for the outermost regions, but the angles for these isophotes are very uncertain. The ellipticity profile (Fig. 13, *bottom*) shows that the isophotes become rounder with increasing radius, although again the fits to the outer regions are more uncertain. The brightest parts of the dwarf halo, however, are consistent with its classification as a dE1,N galaxy.

The dwarf nucleus is spatially unresolved with the present data. Its magnitude and color have been determined by computing the excess above the best exponential fits to the surface brightness profiles described above. However, the corresponding uncertainties are large, since the magnitude is very dependent on the model assumed for the underlying galaxy light (and it is not clear which model is the "correct" one). Here we adopt magnitudes based on an exponential fit ($n = 1$) to the *inner* regions of the profile ($5'' < r < 40''$). Out to a radius of 7″, we derive $V_{\rm nuc} = 17.50 \pm 0.03$ and $(B-V)_{\rm nuc} = 0.90 \pm 0.03$. Similarly, the excess above the King model gives $V_{\rm nuc} = 17.2 \pm 0.2$ and $(B-V)_{\rm nuc} = 0.94 \pm 0.01$. The color of the nucleus is the same (within the errors) as that of the surrounding galaxy light, consistent with observations of most dwarf galaxies to date (Caldwell & Bothun 1987; Cellone et al. 1994).

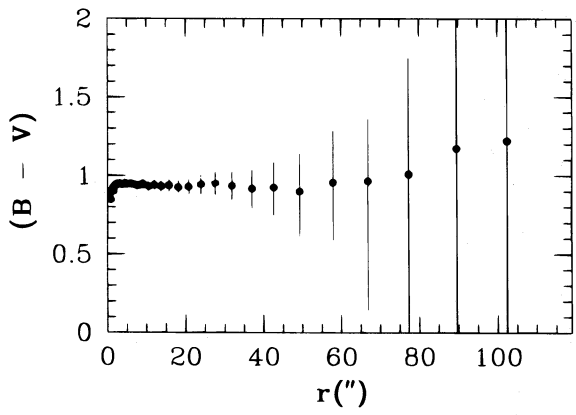

FIG. 12.—Colors of the galaxy isophotes, where $(B-V) = \mu_B - \mu_V$

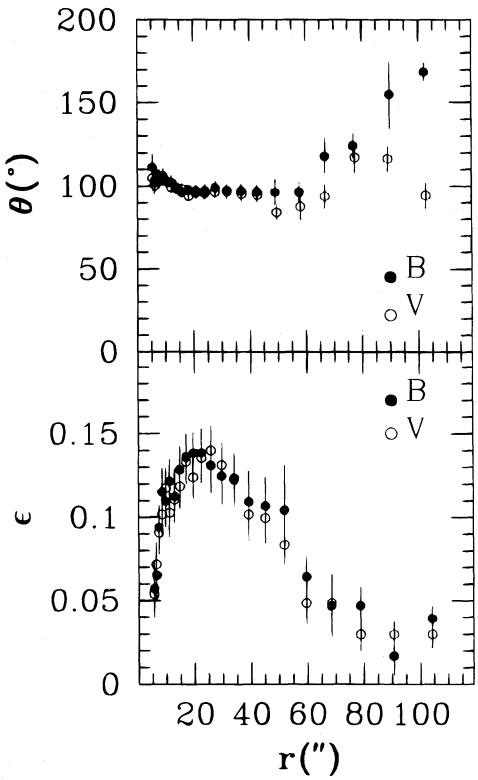

FIG. 13.—(*top*) Position angle profile of the galaxy isophotes for *B* (*filled circles*) and *V* (*open circles*). Here $\theta = 0°$ corresponds to position angle north, and 90° east. (*bottom*) Ellipticity profile of the galaxy isophotes for *B* (*solid circles*) and *V* (*open circles*). Only data for $r > 5''$ have been plotted for both graphs.

An upper limit to the size of the nucleus can be set by the stellar profile FWHM; at $d \sim 11$ Mpc, the half-light radius of the nucleus can be no more than 43 pc. The luminosity of the nucleus is $M_V \sim -12.8$ (using the excess above the exponential fit) or $L \sim 10^7 L_\odot$. This is over 2 mag more luminous than the most massive globular clusters and suggests that the nucleus did not form from the infall of globular clusters (see § 4).

REFERENCES

Ajhar, E. A., Blakeslee, J. P., & Tonry, J. L. 1994, AJ, 108, 2087
Binggeli, B., & Cameron, L. M. 1991, A&A, 252, 27 (BC91)
Binggeli, B., Tarenghi, M., & Sandage, A. 1990, A&A, 228, 42
Bridges, T. J., Hanes, D. A., & Harris, W. E. 1991, AJ, 101, 469
Brodie, J. P., & Huchra, J. P. 1991, ApJ, 379, 157
Buonanno, R., Corsi, C. E., Fusi Pecci, F., Hardy, E., & Zinn, R. 1985, A&A, 152, 65
Burstein, D., & Heiles, C. 1984, ApJS, 54, 33
Caldwell, N. 1983, AJ, 88, 804
Caldwell, N., Armandroff, T. E., Seitzer, P., & Da Costa, G. S. 1992, AJ, 103, 840
Caldwell, N., & Bothun, G. D. 1987, AJ, 94, 1126
Cellone, S. A., Forte, J. C., & Geisler, D. 1994, ApJS, 93, 397
Chaboyer, B. 1994, in Dwarf Galaxies, OHP/ESO Workshop, ed. G. Meylan & P. Prugniel (Garching: ESO), 485
Ciardullo, R., Jacoby, G. H., & Tonry, J. L. 1993, ApJ, 419, 479
Couture, J., Harris, W. E., & Allwright, J. W. B. 1990, ApJS, 73, 671
Da Costa, G. S. 1992, in IAU Symp. 149, The Stellar Populations of Galaxies, ed. B. Barbuy & A. Renzini (Dordrecht: Kluwer), 191
Da Costa, G. S., & Armandroff, T. E. 1995, AJ, 109, 2533
Da Costa, G. S., & Mould, J. R. 1988, ApJ, 334, 159
Davidge, T. J. 1994, AJ, 108, 2123
Dekel, A., & Silk, J. 1986, ApJ, 303, 39
de Vaucouleurs, G., de Vaucouleurs, A., Corwin, Jr., H. G., Buta, R., Paturel, G., & Fouque, P. 1991, Third Reference Catalogue of Bright Galaxies (Berlin: Springer)
De Young, D. S., Lind, K., & Strom, S. E. 1983, PASP, 95, 401
Durrell, P. R., Harris, W. E., & Geisler, D. 1996, in preparation
Ferguson, H. C., & Binggeli, B. 1994, A&A Rev., 6, 67
Ferguson, H. C., & Sandage, A. 1989, ApJ, 346, L53
Fleming, D. E. B., Harris, W. E., Pritchet, C. J., & Hanes, D. A. 1995, AJ, 109, 1044
Ford, H. C., Jacoby, G., & Jenner, D. C. 1977, ApJ, 213, 18
Freedman, W. L., et al. 1994, Nature, 371, 757
Freeman, K. C. 1993, in ASP Conf. Ser. 48, The Globular Cluster-Galaxy Connection, ed. G. H. Smith & J. P. Brodie (San Francisco: ASP), 608
Graham, J. A. 1982, PASP, 94, 244
Hanes, D. A., & Harris, W. E. 1986, ApJ, 304, 599
Harris, W. E. 1983, PASP, 95, 21
———. 1986, AJ, 91, 822
———. 1990, PASP, 103, 32
———. 1991a, ARA&A, 29, 543
———. 1991b, PASP, 103, 32
———. 1993, in ASP Conf. 48, The Globular Cluster–Galaxy Connection, ed. G. H. Smith & J. P. Brodie (San Francisco: ASP), 472
———. 1995, in IAU Symp. 164, Stellar Populations, ed. P. C. van der Kruit & G. Gilmore (Dordrecht: Kluwer), 85
Harris, W. E., Allwright, J. W. B., Pritchet, C. J., & van den Bergh, S. 1991, ApJS, 76, 115
Harris, W. E., Harris, G. L. H., & McLaughlin, D. E. 1996, in preparation
Harris, W. E., & Pudritz, R. E. 1994, ApJ, 429, 177 (HP94)
Harris, W. E., & van den Bergh, S. 1981, AJ, 86, 1627
Hodge, P. W. 1973, ApJ, 182, 671
———. 1974, PASP, 86, 289
———. 1976, AJ, 81, 25
Jacoby, G. H., et al. 1992, PASP, 104, 599
Jedrzejewski, R. I. 1987, MNRAS, 226, 747
Kauffmann, G., White, S. D. M., & Guideroni, B. 1993, MNRAS, 264, 201
King, I. R. 1966, AJ, 71, 64
Kron, R. G. 1980, ApJS, 43, 305
Landolt, A. U. 1983, AJ, 88, 439
———. 1992, AJ, 104, 340
Larson, R. B. 1990, PASP, 102, 709
———. 1992, in Star Formation in Stellar Systems, ed. G. Tenorio-Tagle, M. Prieto, & F. Sanchez (Cambridge: Cambridge Univ. Press), 125
Lee, M. G., Freedman, W. L., & Madore, B. F. 1993, AJ, 106, 964
McLaughlin, D. E. 1994, PASP, 106, 47
———. 1995, AJ, 109, 2034
McLaughlin, D. E., Harris, W. E., & Hanes, D. A. 1994, ApJ, 422, 486
McLaughlin, D. E., & Pudritz, R. E. 1996, ApJ, 457, 578
McLaughlin, D. E., Secker, J., Harris, W. E., & Geisler, D. 1995, AJ, 109, 1033
Peletier, R. F., Davies, R. L., Illingworth, G. D., Davis, L. E., & Cawson, M. 1990, AJ, 100, 1091

Peterson, R. C., & Caldwell, N. 1993, AJ, 105, 1411
Pierce, M. J., Welch, D. L., McClure, R. D., van den Bergh, S., Racine, R., & Stetson, P. B. 1994, Nature, 371, 385
Searle, L., & Zinn, R. 1978, ApJ, 225, 357
Secker, J. 1992, AJ, 104, 1472
Secker, J., Geisler, D., McLaughlin, D. E., & Harris, W. E. 1995, AJ, 109, 1019
Secker, J., & Harris, W. E. 1993, AJ, 105, 1358
Stetson, P. B. 1992, in ASP Conf. Ser. 25, Astronomical Data Analysis Software and Systems I, ed. D. M. Worral, C. Biemesderfer, & J. Barnes (San Francisco: ASP), 297
Stetson, P. B., Davis, L. E., & Crabtree, D. R. 1990, in ASP Conf. Ser. 8, CCDs in Astronomy, ed. G. H. Jacoby (San Francisco: ASP), 289
Surdin, V. G., & Charikov, A. V. 1977, Soviet Astron., 21, 12
Tully, R. B. 1982, ApJ, 257, 389
Vader, J. P. 1986, ApJ, 305, 669
Vader, J. P., & Chaboyer, B. 1994, AJ, 108, 1209
Vader, J. P., & Sandage, A. 1991, ApJ, 379, L1
Vader, J. P., Vigroux, L., Lachieze-Rey, M., & Souviron, J. 1988, A&A, 203, 217
van den Bergh, S. 1991, PASP, 103, 1053
Yoshii, Y., & Arimoto, N. 1987, A&A, 188, 13
Young, C. K., & Currie, M. J. 1994, MNRAS, 268, L11
Zepf, S. E., Ashman, K. M., & Geisler, D. 1995, ApJ, 443, 570
Zinn, R. 1985, ApJ, 293, 424
———. 1993, in ASP Conf. Ser. 48, The Globular Cluster–Galaxy Connection, ed. G. H. Smith & J. P. Brodie (San Francisco: ASP), 302